uation research programs should therefore be expanded and their results used in operational systems.

References and Notes

1. R. B. Thompson and A. G. Evans, *IEEE Trans. Sonics Ultrasonics* **SU-23**, 292 (1976).
2. N. Patton, Interdisciplinary Program for Quantitative Flaw Definition, contract F33615-74-C-5180, report for the period of 1 July 1975 to 30 June 1976.
3. C. F. Ying and R. Truell, *J. Appl. Phys.* **27**, 1086 (1956).
4. J. E. Gubernatis, E. Domany, J. A. Krumhansl, *ibid.* **48**, 2804 (1977); *ibid.*, p. 2812.
5. J. E. Gubernatis, unpublished report.
6. V. V. Varadan and V. K. Varadan, Interdisciplinary Program for Quantitative Flaw Definition, contract F33615-74-C5180, report for the period 1 July 1977 to 30 June 1978.
7. B. R. Tittmann and W. L. Morris, personal communication. Gubernatis *et al.* (*4*) and Gubernatis (*5*) formulated the theory.
8. M. F. Whalen and A. N. Mucciardi, Interdisciplinary Program for Quantitative Flaw Definition, contract F33615-74-C5180, report for the period 1 July 1977 to 30 June 1978.
9. J. E. Gubernatis, J. A. Krumhansl, R. M. Thomson, Materials Research Council Summer Conference, University of Michigan, Ann Arbor, contract MDA903-76C, 0250, preliminary report, 1976.
10. B. Budiansky and J. R. Rice, *J. Appl Mech.* **45**, 453 (1978).
11. B. A. Auld, *Wave Motion* **1**, 3 (1979).
12. G. S. Kino, *J. Appl. Phys.* **49**, 3190 (1978).
13. M. T. Resch, B. T. Khuri-Yakub, G. S. Kino, J. S. Shyne, *Appl. Phys. Lett.* **3**, 182 (1979).
14. J. D. Achenbach and A. K. Gantesen, *J. Acoust. Soc. Am.* **61**, 413 (1977).
15. J. B. Keller, *J. Appl. Phys.* **28**, 426 (1957).
16. L. Adler, Interdisciplinary Program for Quantitative Flaw Definition, contract F33615-74-5180, report for the period 1 July 1977 to 30 June 1978.
17. B. Tittmann, *Appl. Phys. Lett.* **33** (8), 6 (1978).
18. Y. Murakami, B. T. Khuri-Yakub, G. S. Kino, J. M. Richardson, A. G. Evans, *ibid.*, p. 685.
19. J. Richardson, personal communication.
20. V. M. Jipson and C. F. Quate, *Appl. Phys. Lett.* **32**, 789 (1978).
21. L. W. Kessler and D. W. Yukas, *Proc. IEEE* **67**, 526 (1979).
22. G. S. Kino, *ibid.*, p. 510.
23. ———, J. B. Hunter, G. C. Johnson, A. R. Selfridge, D. M. Barnett, G. Herrmann, C. R. Steele, *J. Appl. Phys.* **50**, 2607 (1974).
24. C. S. DeSilets, J. Fraser, G. S. Kino, *IEEE Trans. Sonics Ultrasonics* **SU-25**, 115 (1978).
25. J. Souquet, P. Defranould, J. Desbois, *ibid.* **SU-26**, 75 (1979).
26. R. B. Thompson, *ibid.* **SU-25**, 7 (1978).
27. B. A. Auld, G. Elston, and D. K. Winslow, paper presented at the 8th European Microwave Conference, Paris, September 1978.

28. The author thanks J. Krumhansl for very helpful comments on this article. Supported by Electric Power Research Institute contract RP609-1, Office of Naval Research contract N00014-78-C-0283, National Science Foundation grant ENG77-28528, Office of Naval Research contract N00014-75-0632, the Center for Advanced Nondestructive Evaluation (operated by the Rockwell International Science Center for the Defense Advanced Research Projects Agency), AFML contract RI74-20773, and NSF contract DMK-76-00726 through the Center for Materials Research at Stanford University.

Radar Measurement of the Upper Atmosphere

James C. G. Walker

In 1958 William E. Gordon suggested that radars then in existence had the power and sensitivity to detect the Thomson scattering of electromagnetic radiation by free electrons in the ionosphere (*1*). That this suggestion was correct was shown almost immediately by Bowles (*2*), who used a powerful radar in Illinois that was originally constructed by the Smithsonian Astrophysical Observatory for the study of the ionized trails produced by meteors in the upper atmosphere. Radar measurement of Thomson scattering offered a means of determining the profile of electron density as a function of height in the ionosphere, and had many advantages over other techniques available at the time. Accordingly, work was begun on facilities specifically designed to exploit the new technique. Gordon led the team that built the Arecibo Ionospheric Observatory (now the National Astronomy and Ionosphere Center) in Puerto Rico, while Bowles led the team that built the Jicamarca Radar Observatory in Peru (*3*).

Summary. In the last two decades large radars have proved to be powerful instruments for the measurement of the properties of the upper atmosphere. These radars were used initially to measure properties of the ionosphere by the Thomson scattering technique at heights above 100 kilometers. Careful interpretation of the power and spectrum of radar echoes yielded data on electron and ion densities and temperatures as well as on bulk motion of the ionospheric plasma, all as functions of height and time. More recent developments have made it possible to measure wind speeds and the structure of turbulence in the stratosphere and mesosphere at altitudes below 100 kilometers.

The first observations of Thomson scattering from the ionosphere were surprising, however. The measured spectrum of the scattered radiation was very much narrower, and therefore much easier to detect in the presence of noise, than Gordon had predicted. Because of this original misunderstanding of the theory of the phenomenon, the instruments constructed at both Arecibo and Jicamarca were considerably more powerful than they needed to be in order to carry out their original missions. Successful measurements of ionospheric properties by the Thomson scattering technique (now called incoherent scatter) have since been made by much smaller radars in France, England, Massachusetts, Canada, and Alaska (*4*). The power of the original incoherent scatter radars at Arecibo and Jicamarca has not been wasted, however, as these instruments have been used as test-beds for the development of new techniques for the measurement of a range of properties of the upper atmosphere wider by far than anyone could have imagined in 1958.

The first extension of the capabilities of incoherent scatter radar was soon realized as theoretical plasma physicists explained the difference between the measured and predicted spectral width of the scattered radiation (*5*). Electrostatic forces between negatively charged electrons and positively charged ions in the ionospheric plasma couple the motions of the electrons to those of the more massive ions. Although it is electrons and not ions that scatter electromagnetic radiation, their motions and therefore the Doppler shift they cause in scattered radiation are constrained by the ions. The spectrum of the scattered radiation has a width that is characteristic of the mean thermal motion of the ions. The shape of the spectrum depends strongly on the ratio of the temperature of the electrons to that of the ions in the plasma that is scattering the radiation, and there is an additional weak dependence of the shape on the proportions of

The author is senior research associate at the National Astronomy and Ionosphere Center, Arecibo Observatory, Arecibo, Puerto Rico 00612.

ions of different molecular mass that are present. Measurements of the spectrum of radiation incoherently scattered from the ionosphere can therefore be analyzed to recover height profiles of electron and ion temperature and ion composition as well as of electron density.

It was these enhanced capabilities that led, during the late 1960's and early 1970's, to the implementation of the incoherent scatter technique at a variety of existing radar installations in Europe and North America. In addition to those at Arecibo and Jicamarca, the instruments at St. Santin in France, Millstone Hill in Massachusetts, and Chatanika in Alaska are still active, a new incoherent scatter radar built by a consortium of European nations is approaching completion in Scandinavia, and plans are being developed for a radar in Greenland near the earth's magnetic pole. Either formally or informally all of these radars operate effectively as resources of the geophysical community (in the United States they would be called National Centers). Their facilities and data are available to all scientists with suitable programs of research.

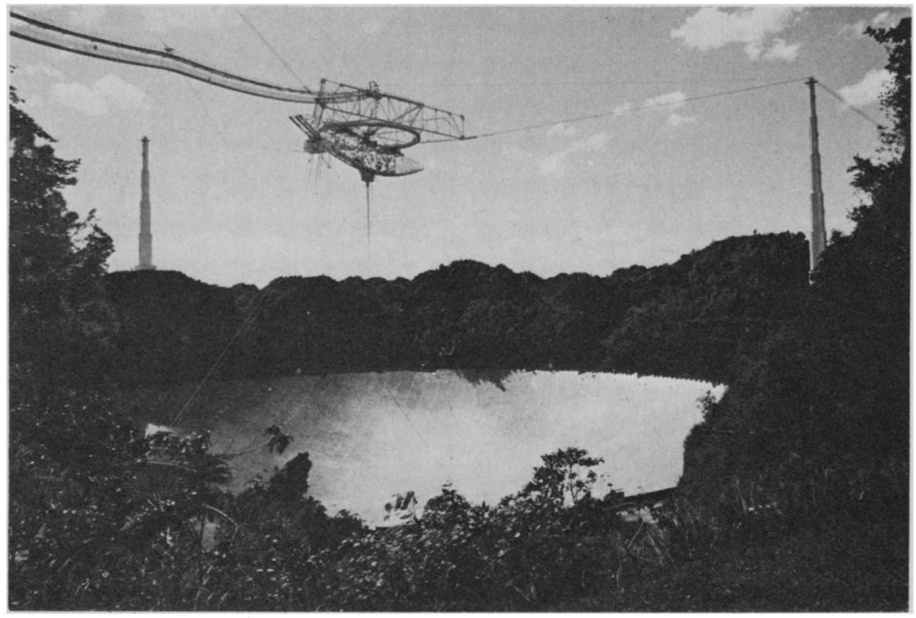

Fig. 1. The Arecibo telescope consists of a fixed reflector, a segment of a sphere, with a diameter of 305 m and an area of 73,000 m^2. Suspended 132.5 m above the reflector are movable carriage houses on which are mounted the radially directed line feeds that collect electromagnetic energy brought to a focus by the reflector. The longest of these feeds (about 30 m) is used in atmospheric radar work at a frequency of 430 MHz. The radar transmitter emits pulses of circularly polarized radiation at peak powers of 2.5 MW and durations adjustable between 2 μsec and 1 msec. The average power output is 150 kW. The radar receiver uses a parametric amplifier with a bandwidth of 10 MHz to achieve a system temperature of about 120 K.

The measurement capabilities of incoherent scatter radars have progressed much beyond ionospheric density, temperature, and composition, as I shall describe below. Particularly useful has been the ability to measure bulk motion of the ionospheric plasma by detection of the Doppler displacement of the scattered radiation from the frequency of the transmitted radiation. This capability has made incoherent scatter radars our principal source of information on the dynamics (winds and electric fields) of the thermosphere, the region of the atmosphere above a height of about 90 kilometers in which most of the ionosphere is located (*6*). New measurement capabilities have been developed at a rate that has accelerated over the years since the first radars were built, and much of this development has been a result not of improvements in transmitters or receivers but of improvements in data processing facilities. The spectrum of a radar echo contains much useful information, but the rate at which data are collected is so high that much of the information is wasted. Atmospheric radar scientists have been using digital electronic devices to cut down on that waste.

A surge of activity in the second half of the 1970's has resulted from the discovery, made at Jicamarca (*7*), that incoherent scatter radars can measure dynamical properties of the stratosphere (15 to 50 km) and mesosphere (50 to 90 km). Facilities dedicated to exploitation of the new measurement capability have been built in West Germany, Colorado, and Alaska. Along with the operating radars I have already mentioned, they promise a contribution to our understanding of the dynamics of the middle atmosphere (stratosphere and mesosphere) as important as the contribution of incoherent scatter radars to our knowledge of the dynamics of the thermosphere.

In this article I describe the measurement capabilities of upper atmosphere radar, drawing on the work of the many scientists who have used the facilities of the Arecibo Observatory.

Approaches to Atmospheric Radar

The experiment of Marconi, in 1901, in which radio signals were sent across the Atlantic Ocean, indicated the presence of a reflecting layer in the upper atmosphere. This layer was interpreted as the ionosphere, a region containing free electrons and ions produced by the action of solar ultraviolet radiation at very short wavelengths (< 1000 angstroms), which photoionizes the constituents of the atmosphere. The refractive index of a plasma (a mixture of equal numbers of ions and electrons) depends on the density and also on the frequency of the electromagnetic wave undergoing refraction. In particular, the wave is completely reflected (the refractive index becomes zero) whenever the wave frequency is equal to the plasma frequency. The plasma frequency is a natural resonant frequency of the plasma, and is dependent only on the density. It is the frequency with which the electron gas would oscillate in the electrostatic field of the ion gas if electrons were pushed out of a region of the plasma, leaving positively charged ions behind, and then released (*5*).

The phenomenon of total reflection of a wave of sufficiently low frequency was exploited in 1924 by Appleton and Barnett and by Breit and Tuve in the first measurements of the properties of the ionosphere [see (*8*)]. A radio wave traveling upward into the ionosphere encounters a region of steadily increasing electron density and plasma frequency until it undergoes reflection at the level where plasma frequency equals the frequency of the wave. The height of the reflecting layer can be determined by measuring the time for a wave to travel up to the ionosphere and back to a radio receiver on the ground.

Out of this early work grew the ionosonde, an atmospheric radar that has been used, principally, to measure the height profile of plasma frequency and thus electron density up to the level of maximum electron density. Before the beginning of the space age, ionosondes were our main source of information on

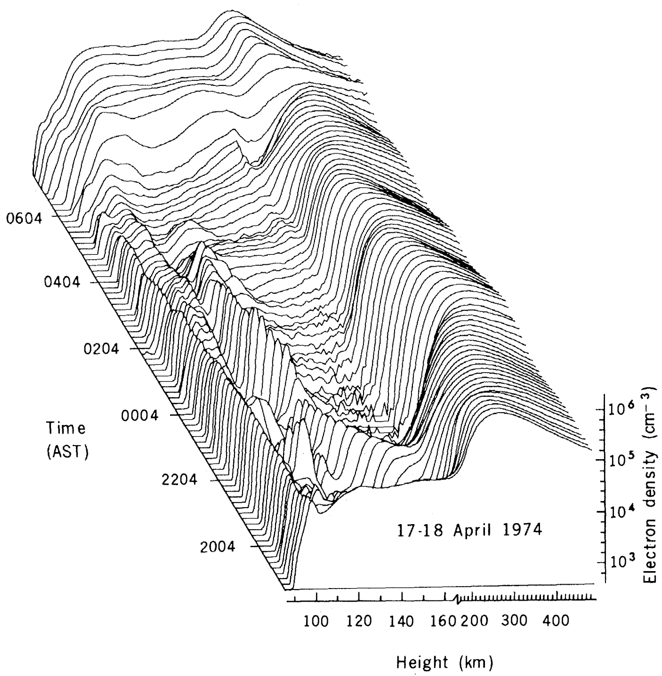

Fig. 2. Electron density profiles measured by R. M. Harper at 15-minute intervals during a particular night at Arecibo (*11*). The density scale is logarithmic, there is a change in height scale at about 170 km, and the time is Atlantic Standard Time, also called Local Time in other figures.

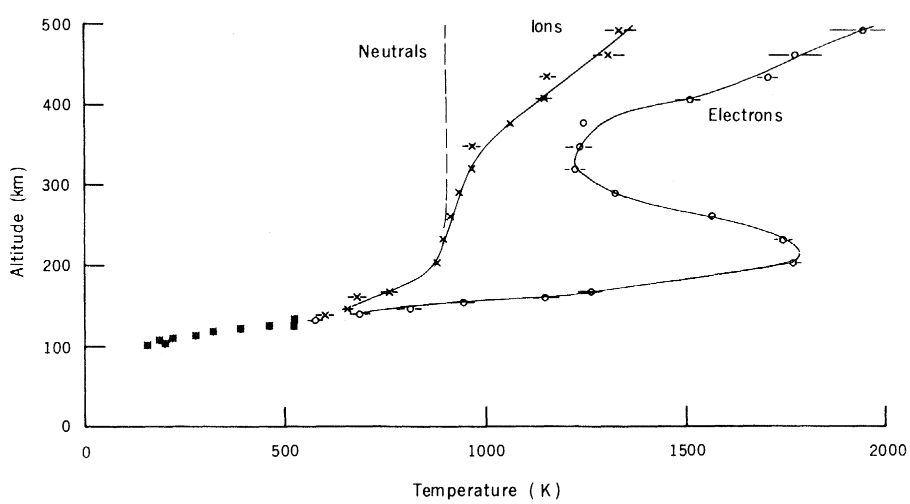

Fig. 3. Charged particle temperatures measured by the incoherent scatter radar at the Arecibo Observatory on 10 August 1974 at 1245 AST. The neutral temperature is inferred from the measured ion and electron temperatures. Actual data points are shown along with statistical error bars (where these exceed 10 K) to illustrate the precision and height resolution that are attainable (*5*). [Courtesy of R. M. Harper]

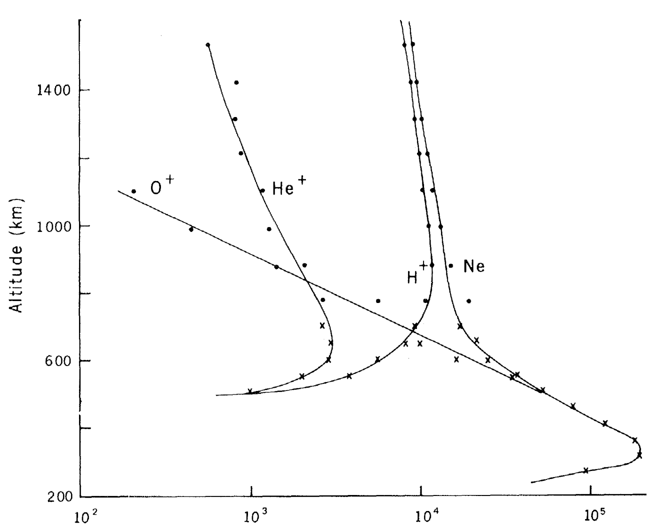

Fig. 4. Ion composition as a function of altitude measured on 10 February 1972 at 2230 by Hagen and Hsu (*26*). Dots and crosses represent the actual data.

the properties of the ionosphere, and they remain the most widely dispersed ground-based instruments today. Perhaps 50 are in operation around the globe, operating generally at frequencies below about 16 megahertz, which is the maximum plasma frequency usually encountered in the ionosphere. Limitations of the HF (high-frequency) sounding technique include its inability to measure electron densities at heights above the maximum, since reflection occurs only as the wave penetrates regions of increasing density, and errors in the height calibration that result from corrections for refraction where the refractive index is not always well determined.

The incoherent scatter radar technique, as originally conceived, promised to overcome these limitations. Because it was believed that it would detect scattering from individual electrons rather than depending on an increase of plasma frequency with height, it would measure density profiles above the maximum as well as below. Errors in height calibration could be avoided by using radar frequencies so much higher than the plasma frequency in the ionosphere that the influence of refraction was negligible (incoherent scatter radars now in operation use frequencies ranging from 50 to 1300 MHz). The technique has fulfilled its promise on both accounts.

Other approaches to atmospheric radar that have proved useful but are not the subject of this article depend on reflection, either total or partial, from sharp spatial gradients in refractive index. The meteor wind technique, for example, measures radar signals reflected from the cylindrical trails of enhanced ionization produced at heights around 95 km by meteor bombardment of the atmosphere. During their short lives these trails are swept along by the wind. Wind speed can therefore be determined by measuring the Doppler shift of the radar echo. There are about ten meteor wind radars in operation around the globe, and together they are our most useful source of information on atmospheric circulation at heights between about 85 and 105 km (*9*). A frequency of operation near 30 MHz is most common as a compromise between the need for detectable echoes from ionized meteor trails (lower frequency waves are more strongly scattered) and the need to avoid reflection from the ionosphere (which would obscure the meteor echoes).

Another example of this class of atmospheric radars are the weather radars that detect scattering from clouds or raindrops in the troposphere (heights less than 15 km). In their simplest form

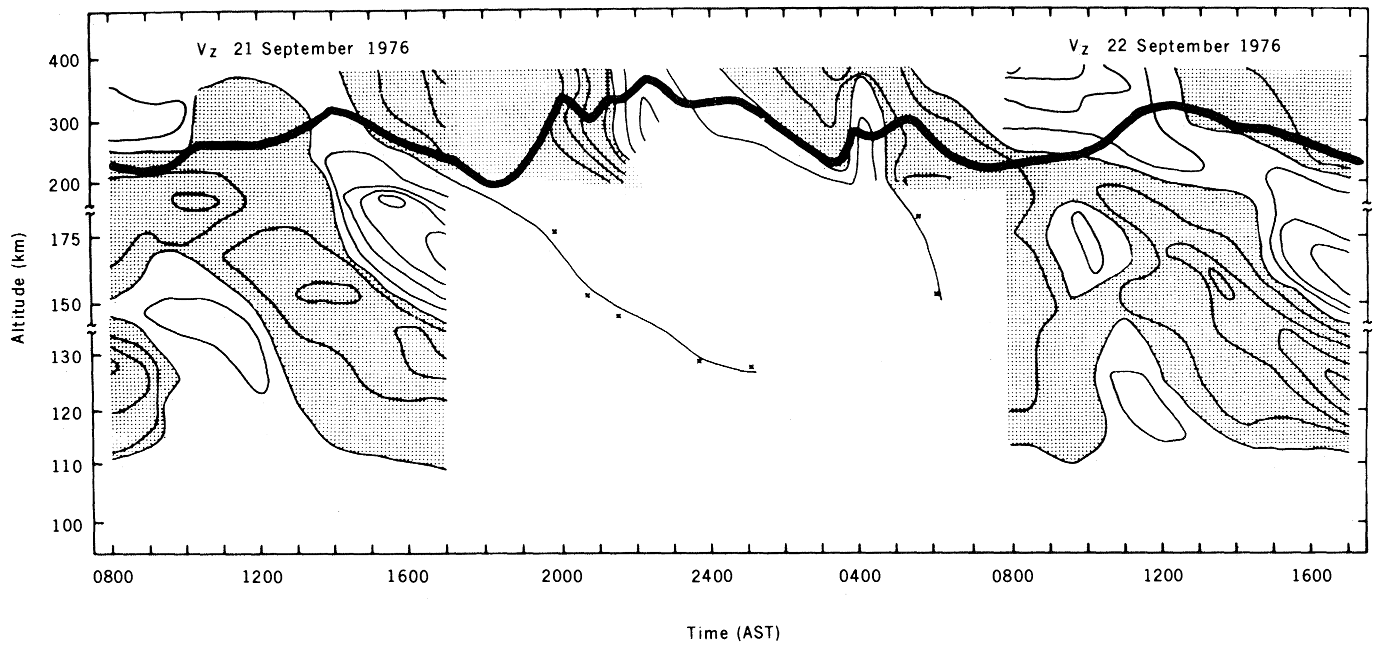

Fig. 5. The vertical ion drift velocity as a function of height and time for two days and the intervening night. The contour interval is 10 m/sec, while the shading denotes downward motion. The heavy line marks the height of maximum electron density, and the crosses show the height of the intermediate layer of enhanced density (*15*).

they locate storms. If spectral analysis is used to measure the velocities of the reflecting particles they also provide valuable information on the dynamics of storms.

Incoherent scattering of radar waves from the atmosphere depends on a different principle (*10*). The scattering is from the very small random fluctuations in density (refractive index) associated with the random thermal motions of the individual particles of the gas. Imagine a spatial Fourier analysis of these random fluctuations at an instant of time. That is, imagine that the instantaneous density distribution is represented by the superposition of an infinite number of density waves of different wavelengths propagating in all directions. Now consider the scattering of a radar wave by the successive peaks of each of these waves. Destructive interference eliminates the radiation scattered by nearly all of the density waves. For two of the waves, however, interference is constructive, and significant scattering is possible. These two waves are those propagating forward and backward along the direction of the incident radiation with wavelengths equal to one-half of the wavelength of the incident radiation (this wavelength criterion applies when the velocity of propagation of the density wave, which might be a sound wave, is negligible compared with the speed of light). This condition for constructive interference is equivalent to the Bragg law that describes the scattering of x-rays from crystal lattices.

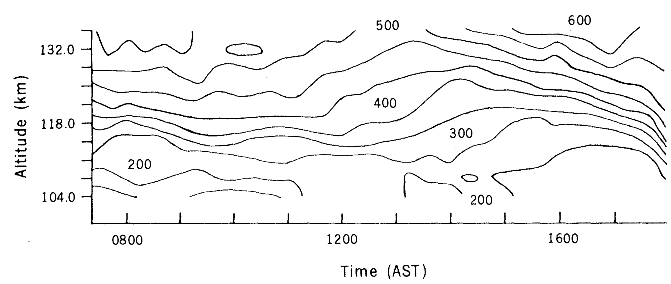

Fig. 6. Ion temperature (degrees kelvin) as a function of height and time in the daytime E region over Arecibo on 4 January 1974. [Courtesy of R. M. Harper]

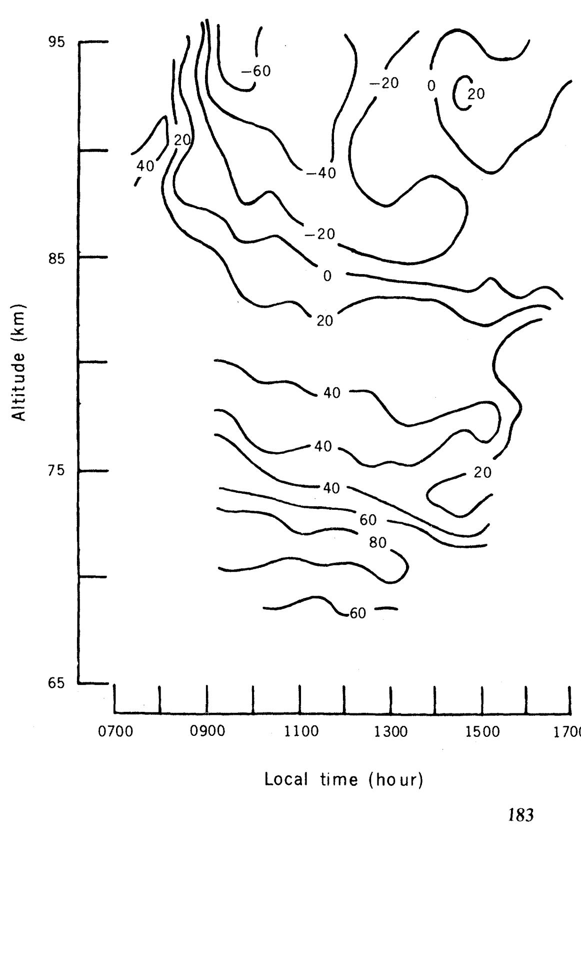

Fig. 7. Eastward wind as a function of height and time in the daytime D region over Arecibo on 8 December 1977. The contour interval is 20 m/sec (*27*).

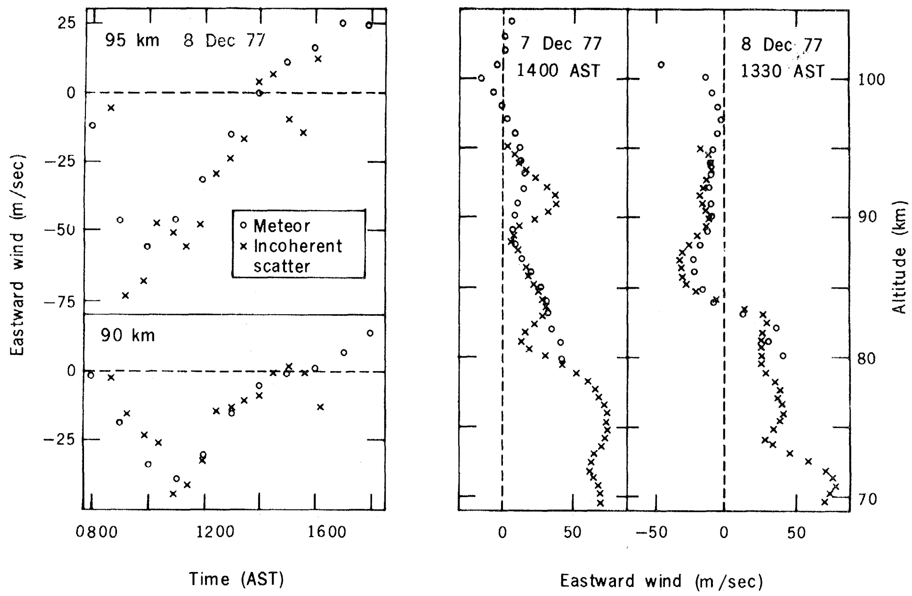

Fig. 8. Comparison of eastward winds measured by meteor wind radar and by incoherent scatter radar. On the left are shown winds as a function of time at two different heights. On the right are winds as a function of height at two different times (*28*).

The incoherent scatter radar, then, detects very small random density fluctuations associated with the finite temperature of the scattering medium. Constructive interference between signals scattered from a large number of fluctuations is what makes the phenomenon detectable in spite of the small amplitude of each individual fluctuation. Random fluctations in the density of neutral molecules scatter radio waves also, but except in special circumstances the scattering is too weak to be detected by radar methods. Random fluctuations in the density of the free electrons in the ionosphere, in contrast, scatter radio waves strongly, and it is this scattering that is measured by incoherent scatter radars.

The density fluctuations correspond to a variety of waves (ion-acoustic waves, Langmuir waves, cyclotron waves) propagating through the ionospheric plasma. Various equilibrium and nonequilibrium processes within the plasma excite these waves, maintaining a steady-state spectrum influenced by dissipative forces. The amplitudes of the waves therefore depend on the properties of the plasma and on their velocities of propagation (governed by the dispersion relation appropriate to each particular type of wave). The radar wave that is scattered from a density wave of appropriate wavelength, propagating along the line of sight of the radar, suffers a Doppler shift in frequency dependent on the velocity of the density wave. Thus measurement of the spectrum of the scattered radiation (amplitude as a function of frequency) provides information on the properties of the plasma (*5, 10*).

In a typical radar experiment a short pulse of radiation is transmitted, and the scattered signal is recorded and analyzed as a function of time after transmission. In this way the properties of the ionospheric plasma are measured as a function of height (one-half the delay time divided by the speed of light). The signal is very weak. Typically, the power scattered in all directions amounts to less than one part in 10^{11} of the transmitted power, whereas less than one part in 10^{6} of the scattered power is collected by the receiving telescope. Thus incoherent scatter radars require large reflectors to collect the scattered radiation and focus it onto the receiver (see Fig. 1). They also require powerful transmitters and sensitive receivers. And even when all of these have been provided it is usually the case that the signal-to-noise ratio is still less than one. What makes the technique feasible is the ability to transmit hundreds of pulses every second and to record and average thousands or millions of returns. Fast data processing equipment is therefore as essential as any of the other components of a radar system. As already noted, improvement in data processing capabilities has been largely responsible for recent gains in the capabilities of upper atmospheric radars.

Ionospheric Properties

Electron density. Incoherent scatter radar was originally proposed as a method to measure height profiles of ionospheric electron density as a function of height. How well the technique has succeeded in this respect is shown in Fig. 2, where successive profiles measured at 15-minute intervals are arranged one behind the other to give an isometric view of ionospheric behavior during a single night at Arecibo (*11*). On the right lies the region of maximum electron density, called the F region. It oscillates up and down in altitude, responding to changes in winds and electric fields that cause vertical motion of the plasma, but it changes little in amplitude. Electron density drops by several orders of magnitude below the F region. At these heights the radar is measuring as few as 300 electrons per cubic centimeter at a range of 150 km. Near 100 km (the E region) are sharp layers of ionization that persist, with some change in amplitude, throughout the night. Density drops precipitously below the E region. A most striking feature is the pronounced layer of enhanced density that emerges out of the F region at the beginning of the night, descending slowly in altitude to disappear quite suddenly around 0400 hours. I shall say more about this layer below. The increase in density at all levels after 0600 hours is caused by sunlight, which produces new ions and electrons by photoionizing neutral atmospheric molecules.

Electron and ion temperature profiles. An example of electron and ion temperature profiles is shown in Fig. 3. These are daytime data. The maximum in electron temperature near 200 km is a consequence of photoionization. Photoionization of atmospheric molecules by solar ultraviolet radiation produces photoelectrons with energies of typically 10 electron volts, much greater than thermal energies (~ 0.1 eV). These photoelectrons travel through the ionospheric plasma, losing energy gradually in collisions with the ambient thermal electrons. The ambient electrons gain, as heat, the energy lost by the photoelectrons. The electron temperature is raised as a result. The thermal electrons lose energy in collisions with the cooler ambient ions. This cooling is particularly rapid near 300 km, where the ion density is at a maximum. A minimum in electron temperature results. The ions, in turn, lose heat as a result of collisions with ambient neutral molecules. At lower altitudes, where the neutral density is relatively large, the thermal coupling between ions and neutrals is close. At higher altitude the neutral density is too low to control the ion temperature closely. Both ion and electron temperatures rise.

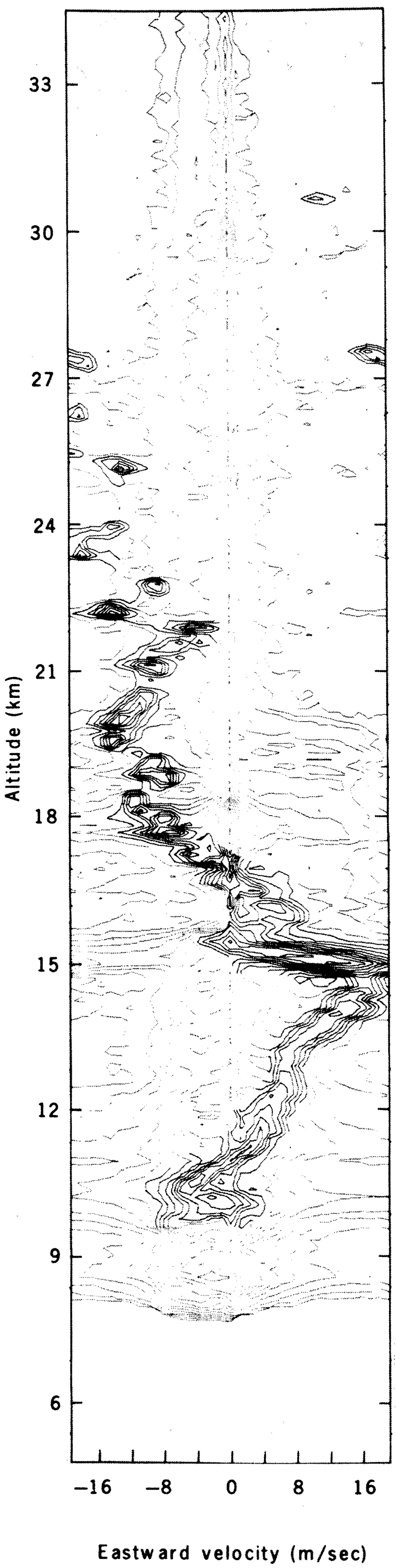

Fig. 9. Radar scattering from atmospheric turbulence as a function of height and frequency, here shown as the eastward wind speed which produces the corresponding Doppler shift in frequency. [Courtesy of R. F. Woodman (*29*)]

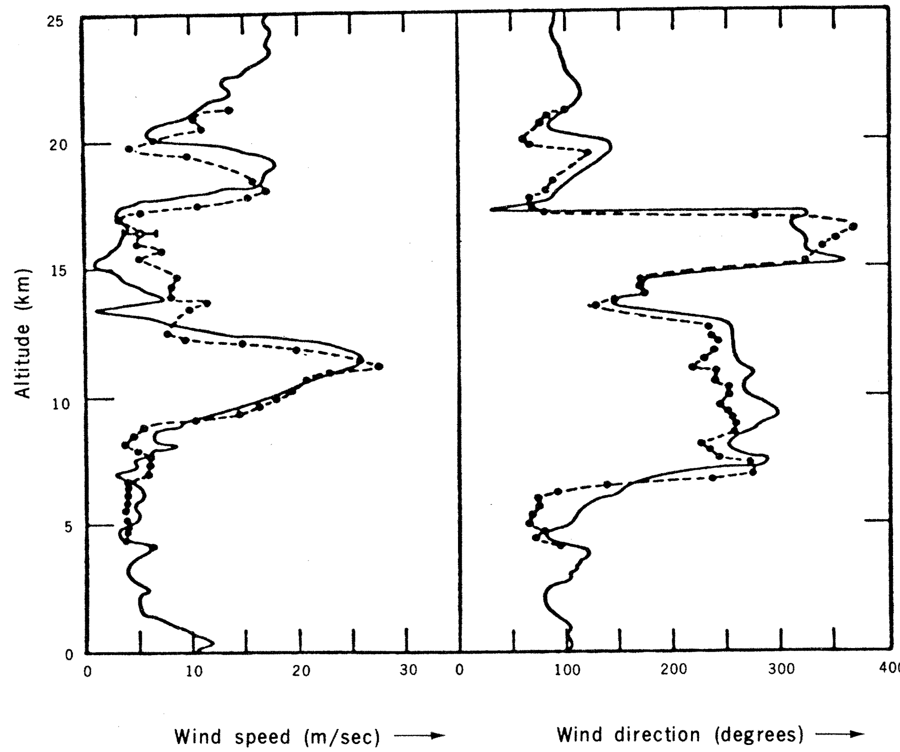

Fig. 10. Comparison of profiles of wind speed and direction derived from the frequency shift of radar echoes from atmospheric turbulence and from the tracking of a rawinsonde balloon, 6 April 1977 (*21*). Broken lines with solid circles indicate radar-derived winds at Arecibo, from 1939 to 2013 hours (60°W); solid lines indicate rawinsonde winds at San Juan, from 1900 to 2051 hours.

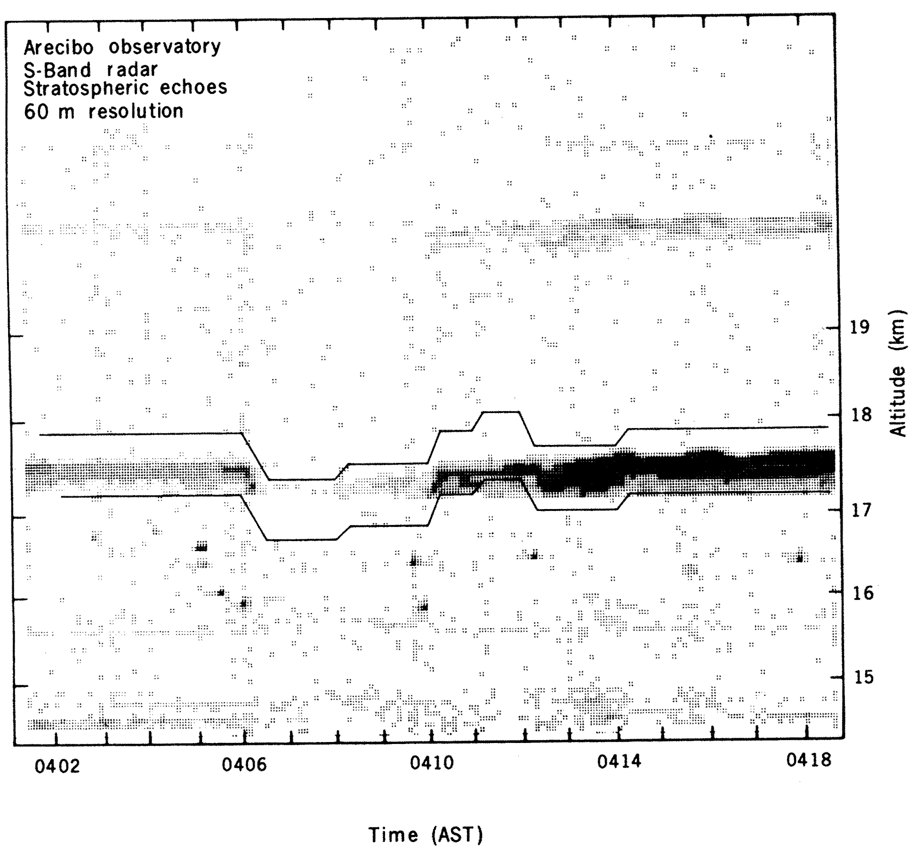

Fig. 11. The power of radar echoes from a layer of turbulence in the stratosphere as a function of height and time. Dark shade corresponds to strong echoes. The horizontal straight lines delimit, approximately, the region of the atmosphere explored by the radar beam. [Courtesy of R. F. Woodman (*29*)]

Heat is removed from the high-altitude plasma by thermal conduction in both ion and electron gases (*12*).

Composition. An example of ion composition measurements extending up to a height of 1600 km is shown in Fig. 4. Below about 700 km the dominant ion is O^+, produced, during the day, by the photoionization of O, the dominant neutral constituent of the atmosphere at F-region altitudes. The density decreases with altitude above the maximum in a balance between the gravitational force on the ions, directed downward, and a force corresponding to the gradient of pressure, directed upward. Hydrogen and helium ion densities decrease with altitude more slowly than oxygen ion density because the gravitational force on them is weaker. The hydrogen ions are produced by a charge exchange reaction between oxygen ions and neutral hydrogen atoms, while the helium ions are produced, during the day, by photoionization of neutral helium. The low-altitude decrease in ion density is caused by recombination reactions, which become more rapid as neutral density increases with decreasing altitude (*13*).

Bulk motions. An important achievement of the incoherent scatter radar technique has been the measurement of the bulk motions of the ionospheric plasma (*14*). The measurement is technically difficult because typical plasma drift velocities are very much smaller than typical ion thermal speeds, so it is necessary to measure a Doppler shift of a spectral feature that is very much smaller than the width of the feature. In spite of the difficulties, all incoherent scatter radars today make drift velocity measurements (*6*). As an example, Fig. 5 shows contours of the vertical component of the ion drift velocity measured on two successive days and the intervening night at Arecibo (*15*). Direct measurement of velocity below 200 km is not possible at night; electron densities are too low.

The data show a remarkable pattern of velocity, alternately upward and then downward, that starts at high altitude and moves steadily downward, repeating itself at 12-hour intervals. This pattern is a consequence of a tidal oscillation in the wind field in the thermosphere. Atmospheric tides are produced by periodic solar heating of the atmosphere. In the thermosphere their amplitudes are so large as to dominate atmospheric dynamics. The winds are horizontal but they cause vertical motion of the ionospheric ions because the ions are constrained by their charge to move only along the lines of force of the geomagnetic field (in the absence of an electric field). Thus the ions slide up along the field lines when the wind blows toward the equator and down along the field lines when the wind blows away from the equator. The downward progression in the phase of the wind field is a characteristic feature of atmospheric tides (*16*).

The heavy line in Fig. 5 shows how the height of maximum electron density changes in response to the slowly oscillating drift velocity of the ions. Similar vertical movements of the F region have already been noted in Fig. 2. Of particular interest are the contours of zero drift which separate an underlying region of upward drift (clear) from an overlying region of downward drift (shaded). These lines mark levels of convergent ion motion, with ions flowing inward from both above and below. Convergent motion produces a sharp layer of enhanced electron density like the layer shown in Fig. 2 that descended out of the F region at the beginning of the night. Electron density data have been used to extend the contours of convergent ion motion in Fig. 5 downward into the nocturnal ionosphere below 200 km where direct velocity measurements are not possible.

Tidal measurements at lower altitudes. Radar measurement can be used to trace the tides to lower altitudes to see how their properties change. In the E region they are most clearly revealed in data on the ion temperature, which at these heights is equal to the neutral temperature, such as those shown in Fig. 6. Although temperature measurements at these heights are possible only during daylight hours, the strong semidiurnal period of the oscillation is readily apparent as is the downward progression in phase. Maximum temperatures occur first at the top of the picture. By the time the maximum has progressed to the lowest altitudes illustrated, the temperature at the highest altitudes has already fallen to a minimum (*17*).

Measurements of the D-region ionosphere. The results I have discussed thus far might be described as resulting from traditional incoherent scatter radar; that is, from regions of moderately large electron density. They are based on measurement of electron and ion temperatures and densities and ion drift velocities in the E and F regions of the ionosphere (heights above 100 km). In the last few years it has become possible to use the power and sensitivity of the Are-

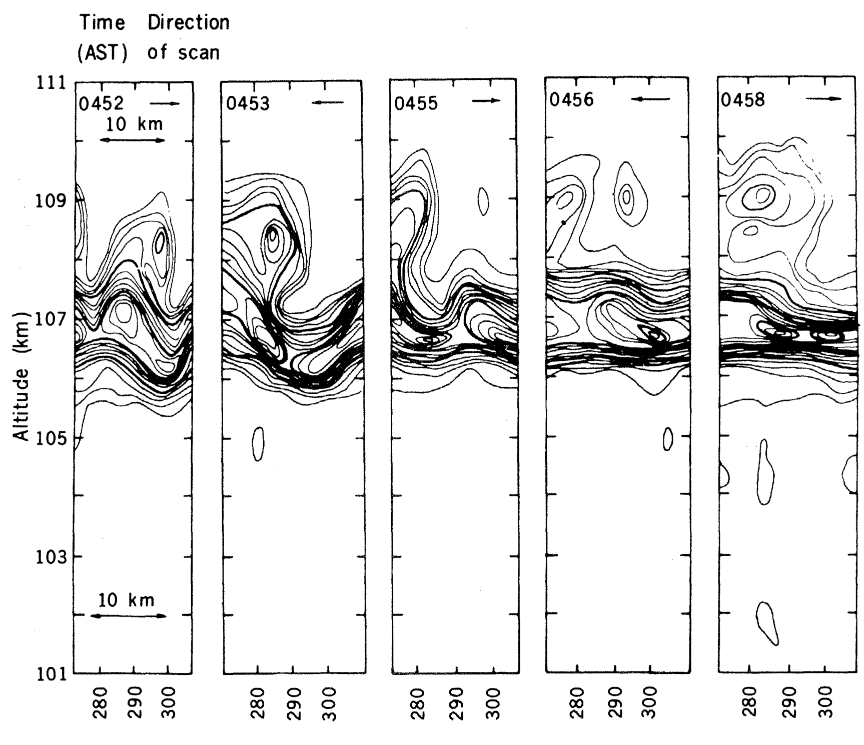

Fig. 12. Successive cross sections of a sporadic E layer measured, at intervals of a minute or two, by determining electron density as a function of height while the radar beam scans back and forth across the sky. A scan takes a little over a minute to complete, so the separation of horizontal and temporal change is not perfect. Contours of electron density are shown with contour intervals of 10^4 electrons per cubic centimeter. The horizontal scale of distance is compressed (*25*). The data were obtained at Arecibo on 17 July 1975.

cibo radar system for incoherent scatter measurements in the D region of the ionosphere, below 100 km, where electron densities are low and the radar return correspondingly weak (*18*). Figure 7 shows contours of the eastward component of the ion drift velocity, which at this altitude is equal to the neutral wind. One-half hour of integration is needed to measure a profile of wind speed at these heights. The height resolution is 600 m. The atmospheric tide is still obvious in these data at heights above about 85 km, as indicated by the downward progression of phase. At lower heights the wind becomes more nearly steady; tidal oscillations no longer dominate the dynamics. Although not obvious in data for a single day, analysis of longer series of data has shown that tides in the D region exhibit a strong diurnal (24 hour) component that is absent in the overlying E region.

The D-region measurements by incoherent scatter radar overlap the height range in which winds can be measured by the meteor radar technique. The new measurement capability therefore provides an opportunity for comparison of the two techniques in order to verify their accuracies and to gain a better understanding of their strengths and weaknesses. Figure 8 presents a comparison of meteor radar and incoherent scatter winds measured within 50 km of one another over Puerto Rico. The agreement is, in general, very good. The discrepancies that exist are readily attributed to differences in the height and time resolutions of the two techniques. Because the meteor radar samples the wind field at random times and random points in height and horizontal position, whenever and wherever appropriate meteors arrive, the data must be smoothed in height and time to yield the wind field. The meteor wind data shown in Fig. 8 were smoothed over several hours in time and several kilometers in height. Although not matching the incoherent scatter technique in height or time resolution, the meteor wind technique offers advantages of economy, both in capital investment and operating cost, and it provides data at night as well as during the day.

Very recent developments have demonstrated the capability of incoherent scatter radar to measure the density of electrons in the D-region ionosphere, the density of negative ions, and the ion-neutral collision frequency, which is proportional to the neutral density (*19*). These measurements will provide much-improved opportunities to explore the chemistry and dynamics of the lowest layer of the ionosphere.

Turbulence

A new approach to the measurement of dynamical properties of the middle atmosphere was developed at the Jicamarca Radar Observatory in 1974 (*7*) as an outgrowth of work at other locations on radar scattering in the troposphere (*20*). Like the techniques already discussed, this technique measures the radar signal scattered by random fluctuations in the refractive index of the atmosphere, and the scattering mechanism is the same. However, it relies not on the very small fluctuations produced by random thermal motions but on the much larger fluctuations produced when turbulence mixes high- and low-density air from different levels of the atmosphere. This technique has made possible the measurement, by means of radar, of the dynamical properties of the lower stratosphere, a region of the atmosphere where conventional incoherent scatter

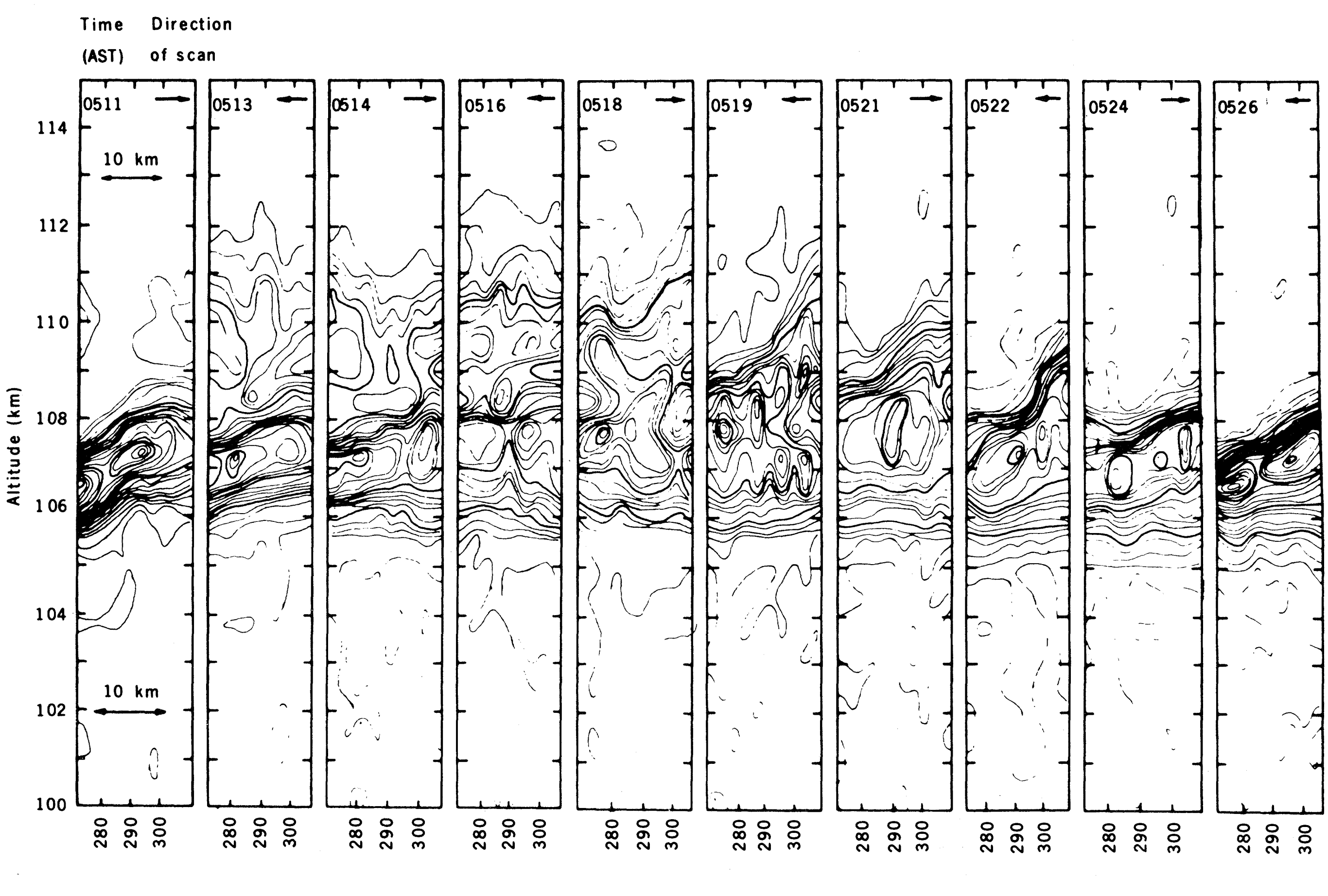

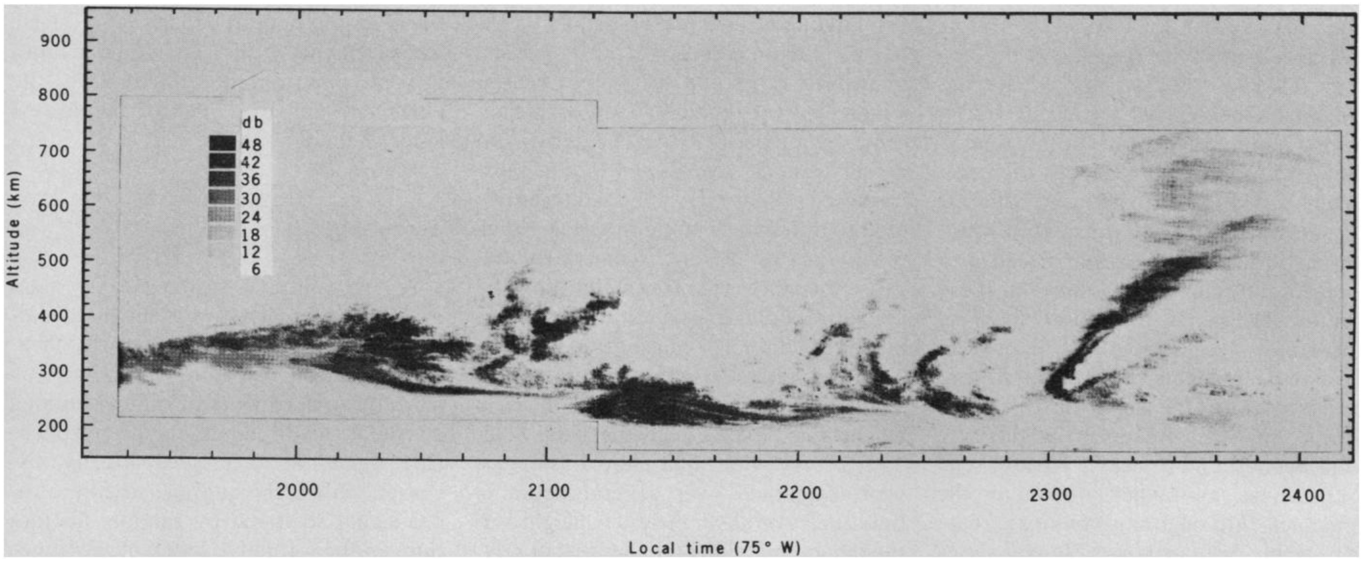

Fig. 13. Radar echoes from turbulence in the ionospheric plasma measured as a function of height and time over Jicamarca, 19 March 1974. Dark shade corresponds to strong echoes (*25*).

radar is powerless because of the absence of free electrons.

Figure 9 shows measurements plotted as contours of scattered power as a function of height (between 9 and 30 km) and frequency. The contour interval is logarithmic, which means that the radar echoes, which appear as an enhanced band moving first to the right and then to the left, are several orders of magnitude more intense than the noise that fills the rest of the figure. The strip up the middle is ground-clutter: echoes caused by stationary objects outside the main beam of the radar. It should be ignored. The variation in the frequency of the radar return with altitude is a consequence of the Doppler shift caused by the wind which carries turbulent irregularities along with it. Figure 10 compares the profile of wind speed as a function of altitude measured by the radar with that deduced by tracking a rawinsonde balloon released from San Juan International Airport, about 80 km away (*21*). The two measurement techniques are in excellent agreement, but rawinsonde balloons are normally released at 12-hour intervals, whereas radar echoes are always present, allowing measurements of upper air wind speed to be made with a time resolution of minutes. Clearly the radar offers a powerful new capability for the study of short-period changes in the wind.

Equally interesting is the information provided by the radar on the distribution of turbulence in the upper troposphere and lower stratosphere. Woodman's data (Fig. 9) show echoes at all heights up to the tropopause, near 15 km. Turbulent irregularities in density are therefore present throughout the upper troposphere. The tropopause itself is marked by very strong turbulence associated with rapid change in wind speed with height (strong shear). In the stratosphere, turbulence becomes increasingly erratic in occurrence until, at the highest levels explored, it appears only in isolated layers separated by as much as 500 m of air devoid of turbulent irregularities in density. The height resolution of these data is 150 m, sufficient to reveal the layered structure of turbulent regions separated by air devoid of turbulence, but not sufficient to resolve the structure of the turbulent layers themselves. For a closer look at an individual layer, a radar of greater bandwidth, capable of finer height resolution, must be used.

Measurements with such a radar are shown in Fig. 11. This figure presents echo power on a logarithmic scale of shades as a function of height and time. The height resolution, corresponding to a single horizontal stripe of shade, is 60 m. These measurements were made in the region of intersection of the beams of separate receiving and transmitting antennas, a region whose upper and lower limits are approximately indicated by the straight lines. Echoes from altitudes much outside this region are of uncertain origin. The measurements show that a layer of stratospheric turbulence is sharply bounded both above and below by air free of density irregularities, that the turbulence is strongest in a layer typically only 180 m thick, and that the strength of the turbulence within the layer varies over height intervals as small as 60 m and during times as short as 20 seconds. There is evidence that layers of turbulence in the stratosphere may be much thinner than 60 m (*23*).

These measurements are so new that a clear physical understanding of the nature of stratospheric turbulence has not yet been achieved. What follows is a tentative account of what may be happening (*23*). First, the stratosphere is so named because it is stably stratified. Vertical displacement of air, such as that associated with turbulence, is opposed by the force of buoyancy. A parcel of air displaced upward is denser than the surrounding medium and tends to return to its original level. Thus turbulence in the stratosphere does not occur spontaneously but is driven by shear in the wind (a vertical change in the horizontal wind speed or direction). When the wind shear is large enough, small perturbations in the flow of the air can be amplified by nonlinear processes that convert vertical differences in horizontal velocity into vertical velocity. This breakdown of laminar flow into turbulence occurs only if the wind shear is at or above a critical value. But, by mixing air from different levels with different speeds, turbulence extracts energy from the wind field, eliminating the shear that was the cause of the turbulence in the first place. So we believe that stratospheric turbulence is sporadic. Shear in the wind field builds up until the critical value is achieved, whereupon the flow breaks down into turbulence. The shear is reduced by the turbulence, but even after their source of energy has disappeared it takes some time for the turbulent motions to die out. Once laminar flow has been reestablished, the wind shear begins to increase again until the whole process is repeated.

We do not yet have observations of the entire life cycle of a layer of stratospheric turbulence, but a remarkable series of radar observations by Miller and Smith (*24*) has shown the sequence of events I have just described taking place in the E region of the ionosphere, at a height of 107 km. To obtain these observations one uses a thin layer of high electron density, called a sporadic E layer, as a tracer of atmospheric motion, much like the thin layer of dye that one might use to trace motions in a laboratory experiment in fluid dynamics. The sporadic E layer is produced by convergent vertical motion of ionospheric ions and electrons that results from wind shear, in the manner described for Fig. 5. Examples of sporadic E layers can be seen on the left of Fig. 2.

Figure 12 shows successive "snapshots" of the horizontal and vertical distribution of the electron density in a sporadic E layer measured by swinging the radar beam in azimuth (*24*). The first five frames of Fig. 12 show an oscillating perturbation in the height of the layer that grows in amplitude until the peak, caught in the higher wind at higher altitude, curls over the trough, much like an ocean wave about to break. The remaining frames of Fig. 12 show what happens when the wave breaks, dispersing the sporadic E layer into a broad band of irregular patches of enhanced electron density, like foam. The sporadic E layer has been engulfed by turbulence. Turbulence is dying out by the end of the sequence of pictures and the sporadic E layer is beginning to form again. The turbulent episode has lasted about 15 minutes, and an approximately equal period of time was occupied by the growth of the wavelike instability that broke down into turbulence. Observations such as these can tell us much about the basic physics of turbulence in stably stratified fluids and also about the effects of turbulence on the dynamical and chemical properties of the upper stratosphere.

I have shown, thus far, measurements of turbulent motions of the neutral atmosphere, but it is possible, under certain conditions, for turbulence to occur also in the ionospheric plasma, at high altitudes where the coupling between the motions of neutral and ionized constituents of the atmosphere is weak. Plasma turbulence can generate very strong fluctuations in electron density, readily detected by atmospheric radar when the geometrical situation is such as to permit constructive interference of the scattered radar signals. Figure 13 shows a particularly spectacular example of scattering from turbulence in the ionospheric plasma measured by Woodman and LaHoz (*25*) at the Jicamarca Radar Observatory, close to the geomagnetic equator. Irregularities in electron density at latitudes near the geomagnetic equator had long been known from a variety of measurement techniques, but their interpretation was obscure until the Jicamarca measurements revealed that they are associated with a disturbance that arises in the F region of the ionosphere and moves upward, at first fast and then more slowly, much like a lighter-than-air balloon. The suggestion, made by Woodman and LaHoz and since confirmed by further experimental and theoretical studies, is that the disturbance is, in fact, associated with bubbles of low-density plasma that originate near the bottom of the ionosphere and rise through the denser overlying ionosphere under the action of buoyant forces. As the bubbles rise, they leave trails of turbulent plasma that look, in the radar data of Fig. 13, much like plumes of smoke.

Conclusion

Radars with the power and sensitivity to measure upper atmosphere properties are too few to provide coverage of the globe adequate for a full understanding of the dynamics of the upper atmosphere. Simpler instruments are needed for the upper atmospheric equivalent of weather stations. The big radars can be used either alone or in conjunction with other instrumentation for comprehensive local study of the details of the dynamical processes that control the properties of the upper atmosphere. For this their capabilities are unmatched.

As our measurement capabilities improve we continue to uncover previously unexpected levels of complexity in the behavior of the upper atmosphere. I have presented here only a few of the surprises that have resulted from recent radar work.

References and Notes

1. W. E. Gordon, *Proc. IRE* **46**, 1824 (1958).
2. K. L. Bowles, *Phys. Rev. Lett.* **1**, 454 (1958).
3. ———, *Science* **139**, 389 (1963); L. M. LaLonde, *ibid.* **186**, 213 (1974).
4. J. V. Evans, *J. Atmos. Terr. Phys.* **36**, 3183 (1974).
5. For a descriptive account of the theory of incoherent scatter radar, see J. C. G. Walker, *Eos* **59**, 180 (1978).
6. J. V. Evans, *Rev. Geophys. Space Phys.* **16**, 195 (1978).
7. R. F. Woodman and A. Guillen, *J. Atmos. Sci.* **31**, 493 (1974).
8. M. A. F. Barnett, *J. Atmos. Terr. Phys.* **36**, 2071 (1974); M. A. Tuve, *ibid.*, p. 2979.
9. R. G. Roper and J. E. Salah, *ibid.* **40**, 879 (1978).
10. P. Bauer, *Phil. Trans. R. Soc. London Ser. A* **280**, 167 (1975).
11. J. S. Shen, W. E. Swartz, D. T. Farley, R. M. Harper, *J. Geophys. Res.* **81**, 5517 (1976).
12. J. C. G. Walker and N. W. Spencer, *Science* **162**, 1437 (1968); R. W. Schunk and J. C. G. Walker, in *Progress in High Temperature Physics and Chemistry* (Pergamon, New York, 1973), vol. 5, p. 1; R. W. Schunk and A. F. Nagy, *Rev. Geophys. Space Phys.* **16**, 355 (1978).
13. H. Rishbeth and O. K. Garriott, *Introduction to Ionospheric Physics*, (Academic Press, New York, 1969); P. M. Banks and G. Kockarts, *Aeronomy* (Academic Press, New York, 1973).
14. R. A. Behnke and R. M. Harper, *J. Geophys. Res.* **78**, 8222 (1973).
15. R. M. Harper, *ibid.* **84**, 411 (1979).
16. S. Chapman and R. S. Lindzen, *Atmospheric Tides* (Gordon and Breach, New York, 1970).
17. R. M. Harper, *J. Geophys. Res.* **82**, 3243 (1977).
18. J. D. Mathews, *ibid.* **81**, 4671 (1976).
19. C. A. Tepley and J. D. Mathews, *ibid.* **83**, 3299 (1978); S. Ganguly, J. D. Mathews, C. A. Tepley, *Geophys. Res. Lett.* **6**, 89 (1979); R. M. Harper, *ibid.* **5**, 784 (1978).
20. K. S. Gage and B. B. Balsley, *Bull. Am. Meteorol. Soc.* **59**, 1074 (1979).
21. D. T. Farley, B. B. Balsley, W. E. Swartz, C. LaHoz, *J. Applied Meteorol.* **18**, 227 (1978).
22. D. Atlas, J. C. Metcalf, J. J. Richter, E. E. Gossard, *J. Atmos. Sci.* **27**, 903 (1970).
23. S. A. Thorp, *Radioscience* **4**, 1327 (1969); J. D. Woods, *ibid.*, p. 1289.
24. K. L. Miller and L. G. Smith, *J. Geophys. Res.* **83**, 3761 (1978).
25. R. F. Woodman and C. LaHoz, *ibid.* **81**, 5447 (1976).
26. J. B. Hagen and P. Y.-S. Hsu, *ibid.* **79**, 4269 (1974).
27. R. M. Harper and K. Fukuyama, unpublished data.
28. These data are unpublished and result from the work of R. Bernard, J. L. Fellous, M. Glass, M. Massebeuf, J. D. Mathews, S. Ganguly, R. M. Harper, J. C. G. Walker, R. A. Behnke, and K. Fukuyama.
29. R. F. Woodman, unpublished data.

30. I am grateful to the scientists who have furnished data illustrated in this paper and who have helped me to understand what the data mean. This paper was written while I was a guest of NASA's Goddard Institute for Space Studies. The National Astronomy and Ionosphere Center is operated by Cornell University under contract with the National Science Foundation. The measurements of stratospheric turbulence were supported by NASA.